British Geological Survey
NATURAL ENVIRONMENT RESEARCH COUNCIL

Wireline Geophysical Logging of the Nirex Deep Borehole in the Sellafield Area: Review of the Status of Wireline Logs and Their Use to Measure Porosity

A report produced for United Kingdom Nirex Limited

Environmental Protection Programme (**ep^2**)

Commissioned Report CR/02/166N

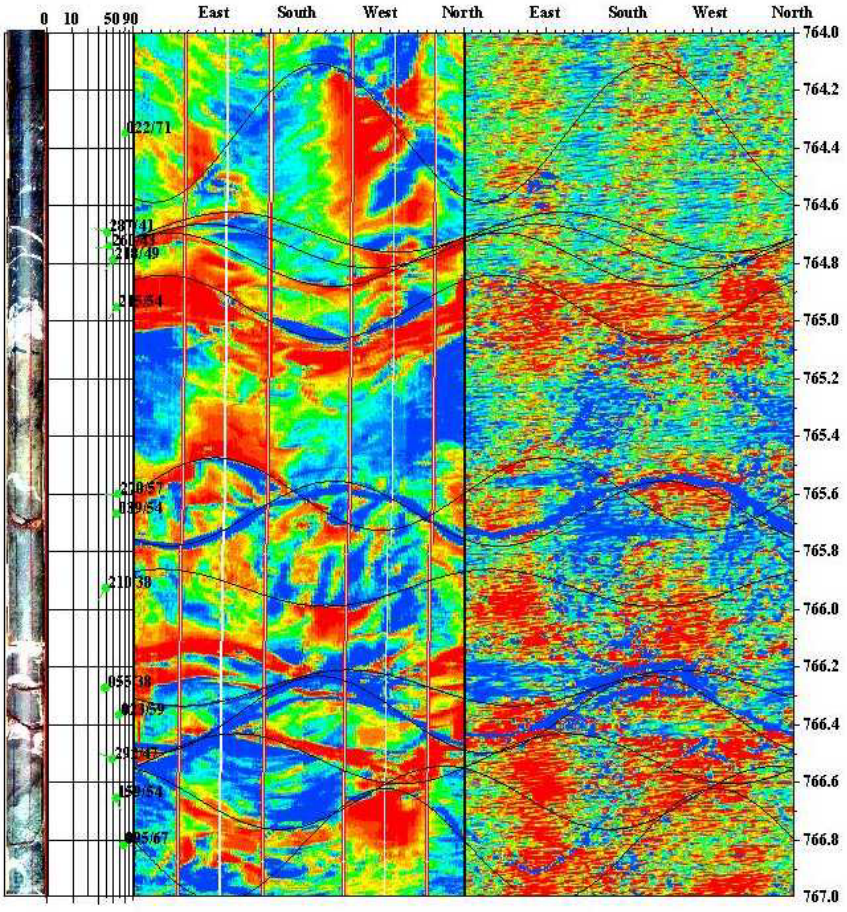

BRITISH GEOLOGICAL SURVEY

COMMISSIONED REPORT CR/02/166N

Wireline Geophysical Logging of the Nirex Deep Borehole in the Sellafield Area: Review of the Status of Wireline Logs and Their Use to Measure Porosity

A report produced for United Kingdom Nirex Limited

C J Evans, R J Cuss and A Kingdon

Front cover

FMS (left) and BHTV (right) Images with scanned core photograph of fractured Borrowdale Volcanic Group rocks, Sellafield Borehole RCF3

Key words

Sellafield; wireline logs; environmental corrections.

Bibliographical reference

EVANS, C.J., CUSS, R.J. & KINGDON, A. 2003. Wireline Geophysical Logging of the Nirex Deep Borehole in the Sellafield Area: Review of the Status of Wireline Logs and Their Use to Measure Porosity. *British Geological Survey Commissioned Report*, CR/02/166N. 27pp.

Keyworth, Nottingham. British Geological Survey 2003

BRITISH GEOLOGICAL SURVEY

The full range of Survey publications is available from the BGS Sales Desks at Nottingham and Edinburgh; see contact details below or shop online at www.thebgs.co.uk

The London Information Office maintains a reference collection of BGS publications including maps for consultation.

The Survey publishes an annual catalogue of its maps and other publications; this catalogue is available from any of the BGS Sales Desks.

The British Geological Survey carries out the geological survey of Great Britain and Northern Ireland (the latter as an agency service for the government of Northern Ireland), and of the surrounding continental shelf, as well as its basic research projects. It also undertakes programmes of British technical aid in geology in developing countries as arranged by the Department for International Development and other agencies.

The British Geological Survey is a component body of the Natural Environment Research Council.

Keyworth, Nottingham NG12 5GG

☎ 0115-936 3241 Fax 0115-936 3488
e-mail: sales@bgs.ac.uk
www.bgs.ac.uk
Shop online at: www.thebgs.co.uk

Murchison House, West Mains Road, Edinburgh EH9 3LA

☎ 0131-667 1000 Fax 0131-668 2683
e-mail: scotsales@bgs.ac.uk

London Information Office at the Natural History Museum (Earth Galleries), Exhibition Road, South Kensington, London SW7 2DE

☎ 020-7589 4090 Fax 020-7584 8270
☎ 020-7942 5344/45 email: bgslondon@bgs.ac.uk

Forde House, Park Five Business Centre, Harrier Way, Sowton, Exeter, Devon EX2 7HU

☎ 01392-445271 Fax 01392-445371

Geological Survey of Northern Ireland, 20 College Gardens, Belfast BT9 6BS

☎ 028-9066 6595 Fax 028-9066 2835

Maclean Building, Crowmarsh Gifford, Wallingford, Oxfordshire OX10 8BB

☎ 01491-838800 Fax 01491-692345

Parent Body

Natural Environment Research Council, Polaris House, North Star Avenue, Swindon, Wiltshire SN2 1EU

☎ 01793-411500 Fax 01793-411501
www.nerc.ac.uk

Foreword

This report is of a study by the British Geological Survey (BGS) under contract from AEA Technology for United Kingdom Nirex Limited.

This report has been prepared, verified and approved for publication by the British Geological Survey. The work was carried out in accordance with the quality assurance arrangements that have been established by the BGS and Nirex and comply with the requirements of ISO 9001.

If you would like to see other reports available from Nirex, a complete listing can be viewed at www.nirex.co.uk, or please write to Corporate Communications at the address below, or e-mail info@nirex.co.uk.

Feedback

Readers are invited to provide feedback to Nirex on the contants, clarity and presentation of this report and on the means of improving the range of Nirex reports published. Feedback should be addressed to:

Corporate Communications Administrator
United Kingdon Nirex Limited
Curie Avenue
Harwell
Didcot
Oxfordshire
OX11 0RH
UK

Or by e-mail to: info@nirex.co.uk.

Contents

FIGURES

TABLES

1 Introduction

As part of the Nirex Safety Assessment and Research Programme and Core Characterisation Programme, extensive measurements have been made of solute diffusivity, porosity, electrical conductivity, formation factor and other properties on core samples of the Borrowdale Volcanic Group (BVG) from the Nirex deep boreholes in the Sellafield area. Systematic differences were found whenever comparisons were made between BVG wireline measurements of porosity and measurements on core plugs in the laboratory, the latter being significantly lower (Brereton, 1997; Brereton *et al.*, 1996; NIREX, 1997). These differences have been attributed to scale of measurement effects, resulting from the small core sample volumes relative to the large rock volumes sampled by wireline logging tools, and also to an in-built bias of core samples towards unfractured rock.

Recent work has led to new methods being developed, based on acoustic impedance measurements, that enable the derivation of porosity, permeability and other properties from either core sample or wireline log data using a common approach (Brereton, 1997; NIREX, 1997). These advances provide a means of making direct correlations between physical properties derived from both the standard techniques and the new methods, based on a range of measurements on core samples, without the added complications of scale of measurement or core sample bias clouding the issue.

The direct comparison between measured and calculated (from acoustic impedance) values of porosity, hydraulic conductivity and grain density proved to be unsatisfactory and inconclusive.

This report is a critical analysis of porosity prediction using acoustic impedance. The aim of this report is to determine the source of inaccuracies in porosity estimate, by looking at the field acquisition of the parameters, the sensitivity of the applied mathematical algorithms and the validity of the underlying assumptions. To undertake this requires a rigorous investigation of the fundamental techniques involved in obtaining the physical property measurements both in the field via wireline logs and in the laboratory. The results of this analysis will then be fed into the algorithm used to calculate acoustic impedance and thus porosity in the report.

Acoustic impedance (AI) is the product of bulk density (ρ_b) and compressional velocity (V_p) and can be determined from both core sample and wireline measurements.

$$AI = V_p \times \rho_b \qquad \textbf{(1)}$$

The following two sections will investigate the accuracy and uncertainties of measuring density and acoustic properties, using standard wireline and laboratory procedures.

2 Wireline logs

2.1 ERROR

Wireline logging attempts to derive from borehole measurements in boreholes *in situ* physical properties equivalent to these derived from measurements that can be routinely performed in the laboratory on rock cores. The logging tools have to be designed to work in a wide range of conditions that are remote from human intervention. The tools are designed to estimate the true parameter value of the formation under investigation. This true parameter value is an intrinsic value and cannot be derived exactly by any physical process. The value derived from measurements is different from the true value and the difference is called the error (Eq.2). Of course one cannot deduce the error otherwise one could deduce the true value. There are two types of error, systematic and random (Eq.3). The systematic error is usually introduced by a human error i.e. mis-calibration, tool design, etc, whereas the random error is due to the inherent variability in measurement techniques.

Measured value = True value + error **(2)**

Error = Systematic error + random error **(3)**

Random error can be reduced, but not entirely eliminated, by such measures as reduced logging speeds or repeat runs whereas systematic error cannot be alleviated unless recognised. Systematic error can unfortunately be the most difficult to detect, unless two separate independent techniques can be applied to derive a parameter. An example of systematic error would be if a logging tool were mis-calibrated on site. Unless very careful records are kept of procedures, this can be impossible to deduce.

Random error on the other hand can often be estimated by an analysis of recorded data sets using Poisson and Gaussian distribution statistics. The estimation of this uncertainty is often defined as the standard deviation and in general logging companies use this figure to define their results. As an example, a quoted value for density of 2.267 ± 0.017 $g.cm^{-3}$ is taken to mean that there is a 68.3% probability that the 'true value' lies between 2.250 and 2.284 $g.cm^{-3}$. What is often forgotten is that this figure does not and cannot include any estimate of systematic error and the true value as stated in the above equations may lie well outside the apparent range. A more detailed account is carried in Log Analyst, 1994.

A commonly overlooked source of error in estimating *in situ* parameters is the effect of drilling the borehole. This clearly disturbs the environment in which the measurements are made. In particular:

- The drilling mud will replace the *in situ* groundwater in the formation in an annulus around the borehole, which is the zone most logs record in.
- The *in situ* stress is altered causing breakouts or fracturing in an anisotropic manner resulting in anisotropic physical properties.
- The temperature profile is altered by the circulating mud.

For borehole logs to work well, there should be an isotropic thick homogenous formation. This rarely occurs in reality and the geological environment around the borehole is typically made up of largely heterogeneous, thin anisotropic formations. This does not mean that wireline logs are of little value, just that they should come with a health warning (which is in

fact printed on most geophysical logs by logging companies). This is because it is possible to over interpret the log data resulting in erroneous conclusions. When interpreting logs it is wise to remember several golden rules:

- The logs may be averaging several metres of formation; some logs will separately identify thin fractures or formations, but others may not resolve these features.
- Always be careful when making comparisons between different boreholes on an absolute scale, as there may be a calibration error.
- The depth of penetration from the borehole wall of the measurement will vary with the tools and the physical properties of the formation.
- The tool may be misreading due to borehole conditions or readings outside tool specifications.
- The azimuthal position can be crucial for some logs such as the sonic as to the exact properties recorded e.g. for the orientation of fractures.

The calculation of the Acoustic Impedance involves the use of two logs, the sonic and the density logs. These logs are acquired on separate logging runs. On each logging run the engineer will attempt to depth match the logs by checking the repeat section Gamma Ray against the first calibrated run of the Gamma Ray. This is done primarily by visual inspection on site and then moving the depth according to this estimated depth difference. Any estimate of the possible errors introduced by this is subjective but anything up to half a meter difference is possible, with more often a quarter of a metre difference. There is also the problem that as the logging run proceeds the cable will stretch variably on each run. So why is this a problem? Any mismatch of the recorded sonic and density log will mean that the derived Acoustic Impedance will have more scatter or 'error'. The best way to illustrate this is to crossplot one log, in this case the Sonic Log from an approximately 100m section of Nirex Borehole RCF3, against itself with a depth shift. Figure 1 demonstrates how, with a progressive depth shift from 0.1 to 1.0 metres, the correlation coefficient dramatically reduces; what should be a perfect fit straight line reduces to a questionable correlation ($R = 0.6904$).

The precise depth matching of geophysical logs is therefore essential to this work and others that utilise more than one log. Serious consideration should be given to ways to improve the present techniques if not in the field then after acquisition.

2.2 DENSITY

This section describes the typical design of the wireline density tools, the principles upon which these measurements are based and, in the following section, an estimate of their inherent accuracy.

The Litho-Density tool used to acquire density data has been developed from the basic Density tool first used some forty years ago. The initial density tool employed a single detector and used a radioactive source, which emitted medium-energy gamma rays (Ellis, 1987) [$^{137}Cs\ \gamma \equiv 0.66$ MeV]. The basic theory is that these gamma rays are absorbed by the rock unit in the formation via the Compton effect, which is proportional to the density of the rock material. Compton scattering is the process of inelastic scattering of gamma rays by interaction with electrons in the rock material, leading to energy transfer from the gamma rays. High-density formation will contain a high density of electrons and produce greater scattering back to the detector, which is shielded from the direct gamma radiation.

$$\rho_b = A - B \times \log(n) \quad \textbf{(4)}$$

where n is the number of counts, and A and B are constants that depend on the source strength and detector efficiency. The detector is pressed against the borehole wall to avoid the variable effect of interaction of gamma rays with electrons in the borehole mud. However it was soon realised that borehole mud cake, which tends to build rapidly around porous formations, was producing anomalous results. Thus a dual detector system was introduced to permit the effect of the mudcake to be evaluated by a short spacing detector and deducted from the long spacing detector count, in which the gamma rays have penetrated deeper into the rock unit.

Another problem was the fact that the early detectors counted all gamma rays. This included back scattered Compton radiation, which because of photoelectric absorbtion is lower energy than the source, but also higher energy from the natural radiation of the formation itself. In the 1970s detector technology improved and the new detectors were able to measure the energy level associated with each count. This permitted the elimination of the non-Compton gamma rays from the detection process.

In order to confirm the response of the Litho-Density tool it is calibrated in the laboratory over a wide range of densities from 1.7 to 3.0 g.cm^{-3} (Keys, 1997).

The Litho-Density is therefore a highly sophisticated tool capable of measuring the apparent density of rock units to within ± 0.02 g.cm^{-3} in optimal conditions. Unfortunately these conditions are rarely if ever found in boreholes.

The biggest error occurs due to poor borehole condition. Caliper measurements are made and if it is assessed that the tool has significant mud between it and the formation, compensation is estimated via a parameter called DRHO. The validity of the estimate is questionable especially in a fractured environment where the borehole profile can change rapidly. Mudcake build up and heavy mud can also cause problems, however this is unlikely to have been a problem in the Nirex deep boreholes.

Porosity is calculated from the Density Log using the following equation (5) and by assuming a clean formation of known solid rock matrix density, ρ_g, with a fluid density, ρ_f, a porosity, ϕ, and the formation bulk density, ρ_b:

$$\rho_b = \phi\rho_f + (1-\phi)\rho_g \quad \textbf{(5)}$$

This method is a good approximation as a quick estimate. However it cannot be considered to be accurate as it relies in particular on the correct input of the matrix density. Further discussion on the errors introduced by a slight variation of this parameter on porosity in such rocks as the BVG of the Sellafield area is discussed in later sections (section 3.5).

2.3 SONIC VELOCITY

The acquisition of sonic velocities in a borehole in its simplest form is just the recording of the time it takes for a pulse of acoustic (sound) energy to be transmitted from a source to a receiver through the materials of the borehole wall. This time is known as the interval travel time and is usually recorded in microseconds per foot (μs.ft^{-1}). As with all geophysics reality does not match such a simple theory and entire theses and books have been written on the complex propagation of seismic waves in boreholes. In this section we will concentrate solely on the factors that control the accuracy and repeatability of sonic measurements.

Throughout the Nirex deep drilling programme in the Sellafield area the Array-Sonic tool was utilised. This tool contains an array of eight receivers spaced six inches apart. A sophisticated technique of waveform processing using all eight arrival waveforms produces a coherency map from which the interval time is deduced. From this time information, the velocities of the compressional and later arrivals of shear and Stoneley waves can be calculated. The Array tool can provide a multitude of other data on transit times for varying distances, which results in effectively different vertical resolutions, mud transit time and amplitude, frequency and energy analysis (Schlumberger, 1989).

Like the density tool it is mainly sensitive to borehole size. However this is compensated for by the reversal of the ray path by using two transmitters. In very slow velocity formations, it is also possible for cycle skipping to occur. This should not have been a problem in the Nirex deep boreholes.

The tool is calibrated before fieldwork and the error in repeatability terms (i.e. precision) is rated as 2 $\mu s.ft^{-1}$. This means that the effective error increases in fast formations such as the Borrowdale Volcanic Group (BVG) at Sellafield. Here for a typical velocity of 5.5 $km.s^{-1}$ the error translates to $\pm$ 0.2 $km.s^{-1}$ or 3.5 % (Keys, 1997).

There are other areas for the introduction of error, such as the velocity in the mud and position of the sonde in the borehole, but these errors have been reduced to minimal levels by recent technology, which checks the mud velocity *in situ* and the distance to the borehole wall.

3 The calculation of porosity from acoustic impedance

This section of the report will investigate the method developed by N.R. Brereton (Brereton, 1997; Brereton *et al.*, 1996) to determine the porosity of bore wall rocks from wireline derived data. This section has been divided into two sections. Firstly the equation for determining porosity is introduced, along with the equations used to determine some of the parameters that cannot be directly or practicably measured. The second part of this section then looks at the algorithm for determining porosity. Analysis was performed to identify the sensitivity of each parameter within the algorithm to identify which of these may be problematic. The analysis simply fed through the algorithm errors of $\pm$ 5 %, representing the 95 % confidence level of experimentation. More realistic errors were also inputted into the algorithm to see what errors are likely to be resultant for data from the Nirex deep boreholes. Throughout the discussion of error propagation through the algorithm, the underlying assumptions are assessed.

Note: At this point, it is important to introduce the authors method for describing errors. It can become confusing when errors on properties that are usually expressed as percentages (such as porosity) are also expressed as percentages. The reader may under or over-estimate errors by misinterpreting these as total errors or fractional errors. To overcome this confusion, the following convention has been adopted:

- Porosity will be introduced as fractions, i.e. a rock with 7 % porosity will be introduced as $\phi = 0.07$.
- Fractional error in porosity will also be introduced as decimals, e.g. a rock with 7 $\pm$ 3 % porosity (i.e. porosity is between 4 and 10 %) will have an error of 0.03 in porosity.

- The percentage error will be introduced as %, i.e. in the above example; the error is 42.9 %.
- Error will also be introduced as a magnification, e.g. if an input error of 5 % is fed into the algorithm and the resultant error in porosity is 10 %, the input error has been amplified by a factor of 2. This will be expressed as ×2.

The consistent use of this convention should allow the reader to follow the error analysis.

3.1 BASIS OF THE ACOUSTIC IMPEDANCE METHOD FOR POROSITY ESTIMATION

The estimation of porosity from acoustic and density log results was introduced in Brereton, 1997 and applied to the BVG in Brereton *et al.*, 1996. It was shown that total porosity could be estimated using:

$$\phi = \frac{\left[\frac{1}{\rho_b V_p} + \frac{q_b}{\rho_b V_p} - \frac{(1+q_g)}{\rho_g V_{pg}}\right]}{\left[\frac{1}{\rho_f V_f} + \frac{q_b}{\rho_b V_p} - \frac{(1+q_g)}{\rho_g V_{pg}}\right]} \qquad \textbf{(6)}$$

where: ϕ = total porosity

ρ_b = bulk density g.cc^{-1}

ρ_g = mineral grain density g.cc^{-1}

ρ_f = pore fluid density g.cc^{-1}

V_p = P (compressional) wave velocity of bulk rock km.s^{-1}

V_{pg} = compressional velocity of the mineral grains km.s^{-1}

V_f = compressional velocity of pore fluid km.s^{-1}

q_b = compressibility index of bulk rock

q_g = compressibility index of grains.

The compressibility index (q) is related to Poisson's ratio and can be expressed as:

$$q = \frac{4}{3\left(\frac{V_p}{V_s}\right)^2 - 4} \qquad \textbf{(7)}$$

where V_s = S (shear) wave velocity of bulk rock km.s^{-1}

Scrutiny of Eq.6 and Eq.7 showed both equations to be mathematically consistent assuming linear elasticity. Porosity can be estimated knowing the density and seismic wave velocities of the bulk rock, granular constituents and fluid. Of these parameters ρ_b, V_p and V_s (thus yielding q_b) are easily measured using wireline-logging methods and ρ_f can be determined from analysis of the pore fluid. The remaining parameters ρ_g, V_f, V_{pg}, V_{sg} and q_g are not easily measurable in the field and require derivation or estimation by other means. The following equations summarise the assumptions made during calculation of porosity:

$$\rho_g = \frac{\rho_b - \rho_f \phi}{(1-\phi)} \quad \textbf{(5)}$$

$$V_s = \frac{V_{sg}}{V_{pg}} \left[V_p - \phi \frac{\rho_f V_f}{\rho_b} \right] \quad \textbf{(8)}$$

Empirical relationships:

$$V_{pg} = 3\rho_g - 1.65 \quad \textbf{(9)}$$

$$V_f = 1.427\rho_f + 0.056 \quad \textbf{(10)}$$

The validity and origin of these equations and approximations is discussed during the sensitivity of Eq.6 during the following sections.

3.2 INVESTIGATING THE SENSITIVITY OF EQUATION 5

Eq.6 was tested to ascertain which parameters cause the largest effects in terms of error propagation. This was done by assuming that all the relationships in the above equations are valid and assigning reasonable values to all parameters. Initially the equation was tested using the laboratory-derived measurements taken on borehole core sample E57. This sample consists of lapilli tuff (unaltered) from the Fleming Hall Formation (Town End Farm member) of the Borrowdale Volcanic Group (BVG) from 813m brt (below rotary table) depth in Nirex Borehole 4 (NSF4).

When applying *Equation 5* to wireline data, it is necessary to use an iterative process to derive ρ_g and V_{pg}. The iterative process is described in more detail later at the end of Section 3.2. When looking at iterative determination of porosity, samples G72 and H87 were also investigated. G72 is a lapilli tuff from the Brown Bank Formation (Seascale Hall member) of the BVG from 1086m brt depth in Nirex Borehole 10A (NSF10A). H87 is a lapilli tuff from the Fleming Hall formation (Longland Farm member) of the BVG from 668m brt depth in Nirex Borehole RCF3. The measured resaturation porosity of samples E57, G72, and H87 were determined to be 0.00292, 0.0296, and 0.0022 respectively (or 0.292 %, 2.96 % and 0.22 %). However, sample E57 recorded a porosity of 0.0384 and 0.001 when measured using the He gas expansion and out-diffusion methods respectively.

Laboratory measurements included values for grain density (ρ_g), which cannot be measured in the borehole. This enabled the results of the method to be tested. The sensitivity of Eq.6 was determined by varying each parameter to 0.95 and 1.05 of their values. This estimated porosity within the limits of the accepted 95 % experimental error margin. Results of this analysis are summarised in Table 1 and Figure 2. The 95 % error margin is the acceptable experimental error limit often quoted in physics, many of the measured parameters, such as V_p, are expected to be more precise when sampled in the field. Parametric input errors of 0.5 to 4.5 % (in 0.5 % steps) were also investigated to look at non-linear error amplification of Eq.6. Initially values for q_b and q_g were identical due to the assumption that the ratio between compression and shear velocity is constant in all materials ($V_s = 0.56\ V_p$). In addition, the effect of having $q_b \neq q_g$ was investigated (Table 2 and Figure 2). Table 3 and Figure 2 show the degree of error propagation using the repeatability values published by Schlumberger; wireline derived velocity and density measurements have standard deviation errors of ± 0.2 km.s^{-1} and ± 0.02 g.cc^{-1} respectively. Initial parameters yield $\phi = 0.02398$, Table 1-Table 3 show the result from these simple tests with corresponding variations recorded as percentage increase or decrease in porosity compared with the 0.02398 result. Changes in total porosity

and the degree of error amplification (as shown in Figure 3) are also displayed. Results are presented graphically in Figure 2 and Figure 3. Table 4 illustrates the non-linear propagation of error through Eq.6 for V_{pg}/V_{sg}, q_b and q_g.

Eq.9 can be modified to:

$$V_{pg} = 2.2\ \rho_g \qquad \textbf{(11)}$$

to improve the agreement between the estimated porosities and the experimentally measured values. The effect of this modification on sensitivity was also thoroughly tested.

When applying Eq.6 to wireline data, it is necessary to use an iterative process to derive ρ_g and V_{pg} using Eq.5 and Eq.9/11. The iteration process includes:

- Measured values of compressional and shear velocities are used to calculate the compressibility index from Eq.7.
- The initial values of grain density and grain velocity are used, together with measured values of bulk density, compressional velocity and pore fluid density to calculate an initial estimate of porosity from Eq.6.
- The first estimate of porosity is then used to calculate new values of grain density from Eq.5 and grain velocity from Eq.9 (or Eq.11), which, in turn, are used to derive a new value of porosity from Eq.6.
- The iterative procedure is repeated until convergence is achieved and stable values of grain density and porosity are produced. In practice, the iteration was run through 25 steps, although convergence tended to result in very small (< reported precision; 4 decimal places) changes in porosity within 10 steps.

Note: Porosity is present on both sides of Eq.6 when Eq.5 is substituted.

As before, all input parameters were investigated for error propagation in *Equation 5* for sample E57, G72 and H87 (Table 5). Table 6 shows the effect of having $q_b \neq q_g$, while Table 7 shows the error propagation for the repeatability quoted by Schlumberger.

3.3 RESULTS OF SENSITIVITY ANALYSIS

The initial test examined the sensitivity of Eq.6 assuming that all variables were known. This would be the case in the laboratory, where most of the parameters can be easily determined (V_{pg} is not easily measured in the laboratory environment). However, this is not the case in the borehole environment, where it is not possible to separately determine the parameters relating to the solid grains (matrix).

Table 1, Figure 2, and Figure 3 show that the porosity calculation is very sensitive to some parameters. All parameters amplify errors, with only V_f resulting in porosity error similar to parameter error (5 %, ×1.1). Table 4 shows that V_{pg}/V_{sg}, q_b and q_g have non-linear error propagation through Eq.6. Errors are amplified more at low errors. The following paragraphs discuss the observed errors in each parameter and consider the validity of the assumptions and the expected accuracy from any measurements.

3.4 FLUID PROPERTIES

Table 1 shows that Eq.6 is sensitive to fluid properties (V_f and ρ_f). A 5 % variation in V_f and ρ_f results in errors of 5.5 % and 11 % respectively in porosity ($\phi = 0.0239 \pm 0.0013$ and ± 0.0026 respectively). The seismic velocity of the fluid is determined from the work of Jones

et al., 1998, applied using Eq.10. The only parameter required in this empirical relationship is the density of the fluid (ρ_f). Eq.10 was derived for V_f at 5 MPa confining pressure (equivalent to pore pressure in the bore environment) and was claimed to be applicable from 0.1 to 20 MPa at 20 °C. A pressure of 20 MPa is equivalent to 2 km depth at Sellafield and represents an acceptable pressure range for the conditions in the Nirex deep boreholes. Jones *et al.*, 1998, showed an almost linear relationship in deriving Eq.10 with variations of only 0.33 % for each 5 MPa increase (approximately 1 % variation at 2 km depth). This relationship takes no account of temperature, which generally increases 15 – 30 °C per kilometre depth. In the North Sea, temperatures can be as great as 180 °C at 6 km depth. Increased temperature will result in a lowering of ρ_f if the fluid is free to expand, or may result in an increased pore pressure if expansion is resisted. A 5 % volume change can occur in NaCl solutions as temperature is increased from 20 – 100 °C at atmospheric pressure (Rogers and Pitzer, 1982). Therefore, neglecting temperature in Eq.10 could result in considerable error in estimation of ρ_f and as a consequence V_f. It could be possible to extend Eq.10 to take into account the effect of temperature; it may also require the inclusion of pore pressure as the degree of resistance to expansion is not currently considered. Pore pressure will be directly related to ρ_f.

The density measured in the laboratory of a groundwater sample from RCF3 was 1.018 $kg.m^{-3}$ (Brereton *et al.*, 1996). The resultant compression velocity of the fluid (calculated from Eq.10) and corrected to ambient pressure in the borehole was 1.504 $km.s^{-1}$. This estimate differs by less than 1.5 % from the measured velocity in the borehole of 1.527 ± 0.013 $km.s^{-1}$. An error of 1.5 % in V_f will translate to an error in ϕ of approximately 1.5 % (×1.1). These observations suggest that the temperature gradient is not significantly affecting the fluid properties in the Nirex boreholes. However, it is possible at other sites that this effect will play a significant role.

3.5 BULK ROCK PARAMETERS

There are three bulk rock parameters [ρ_b, V_p, q_b] within Eq.6, of which ρ_b and V_p can be measured easily in the field (see Section 2). The compressibility index q is derived from V_p and V_s. As V_s is not always routinely measured in the field, it can be derived from a (the ratio of V_p to V_s). However, V_s was measured routinely at Sellafield.

As shown by Table 1 and Figure 2, Eq.6 is very sensitive to errors in all of these parameters. A 5 % error in V_p or ρ_b can result in 40 – 45 % error in porosity (ϕ = 0.0143 to 0.0364 %, for an initial value of 0.023%), although error in V_p in low porosity crystalline rocks is expected to be much less than 5 %. Clearly this level of error amplification (×8.4) is extreme. Eq.6 appears less sensitive to the ratio of V_p to V_s (a). Only ~7 % error occurs from 5 % variation in a (×1.6). However, Christensen (1989) showed that a can be highly variable, being as high as 0.68 for quartz and as low as 0.49 for zircon. A value of a = 0.68 results in a porosity of 0.0359 (50 % overestimate). It is thus advised that V_s be measured whenever possible and, where not available, laboratory-based measurements should give a good approximation. Shear wave velocity is routinely measured in the field and thus the use of a has become almost redundant.

As stated earlier for sonic logs, transit times have a repeatability (precision) of ± 0.2 $km.s^{-1}$ (often still quoted in Imperial measurements as ± 2 $\mu s.ft^{-1}$). For the example quoted in Table 1 (V_p = 5.62 $km.s^{-1}$) this level of precision equates to approximately 3 % error, which is well within the acceptable 5 % experimental error limit. The sensitivity of Eq.6 shows that 3 % error in V_p results in 25 % error in ϕ (×8.5).

For the density logs, as investigated earlier, has repeatability of ± 0.025 g.cc^{-1} equating to less than 1 % error. This again is significantly less than the acceptable 5 % experimental error margin. The sensitivity of Eq.6 shows that 1 % error in ρ_f results in 2.2 % error in ϕ (± 0.0027, ×2.2).

3.5.1 The compressibility index, *q*

Brereton, 1997, introduced Eq.6 with terms for compressibility indices for bulk rock and mineral grain, q_b and q_g respectively. In the later application of the equation, lack of data led to the use of only a single q term, i.e. it was assumed that $q_b = q_g$. The compressibility modulus is derived from elasticity theory and is mathematically correct assuming perfect linear elasticity. However, rocks are far from perfect elastic materials and do not behave in the same ways as metals or other materials, generally due to their composition. In most cases, rocks consist of a number of different grains/crystals of varying physical properties. The mathematics of Eq.7 for a perfect material would result in $q_b = q_g$ as V_p/V_s (a) would equal V_{pg}/V_{sg} (a_g). In geomaterials, it is likely that $q_b \neq q_g$ especially at low confining pressures when compaction can be heterogeneous within the bulk sample. Considerable changes in seismic velocity occur at low pressures as fractures begin to close, until at a given pressure a linear increase in velocity is predicted from linear elasticity (Birch, 1960, 1961; Nur and Simmons, 1969). Christensen, 1996, showed that the ratio of q_g to q_b can range from about 0.74 to 1.16 with an overall mean of about 1.0 (0.996 ± 0.11). Although the assumption that $q_g = q_b$ can be supported from this observation, it is worth noting that the spread about the mean is considerable: variations of 5 % and 10 % between q_b and q_g result in 17 % and 33 % error in ϕ respectively (ϕ = 0.0239 ± 0.0042, 0.0079 respectively). This illustrates that separate terms for q_b and q_g are necessary, although this does require knowledge of both V_p/V_s and V_{pg}/V_{sg}.

Error propagation through Eq.6 of q is non-linear and has a power-law relationship, as shown in Table 4. Error amplification is greatest at lower error margins and reduces to about ×3 by 5 % input error.

The presence and nature of cracks also influence the above effect. The compression wave velocity V_p and shear velocity V_s are both markedly decreased by the presence of dry cracks (Anderson *et al.*, 1974; Paterson, 1978). The effect is greater in V_p than V_s which leads to a decrease in a. This is further exacerbated when fractures show clear preferential alignment. V_s tends to be unaltered by fracture direction, whereas V_p can dramatically change. When cracks are filled with liquids such as water, the effect on V_p is largely removed and tends to increase a. Hadley, 1975, showed that a measured normal to specimen axis rose significantly as the rock dilated. These general observations suggest that a and a_g are not equal depending on deformation states and styles. As V_s has been calculated using Eq.8, which includes a_g and does not consider variations associated with fracture populations, there could be error introduced by this assumed relationship.

The error associated with q and a is difficult to quantify using the data available from the Nirex deep boreholes. During the laboratory investigation, shear wave velocity was not recorded due to the preparation method of the samples. It is unlikely that the above-discussed phenomena would be identified due to the fact that test cores are generally taken from intact portions of the total core. Changes in V_p/V_s for similar materials with different fracture populations are unlikely to be routinely tested in the laboratory. In the field, it is clearly possible to observe changes in the V_p/V_s ratio. Brereton, 1997, showed the correlation between V_p and V_s and the corresponding acoustic impedance. While a general trend is observed, there is considerable spread about this trend. It would even be possible to identify 2

linear trends within the data, one below V_p = 4.5 km.s^{-1}, the other above this velocity. This illustrates that it is necessary to have measurements of both compression and shear wave velocities to reduce errors in porosity determination. The lack of shear wave velocity makes it difficult to identify the source in differences observed between field and laboratory based porosity estimates. The observations of Paterson, 1978, suggest that error could be introduced through the terms q_b and q_g.

3.5.2 Predicted V_s

Brereton, 1997, looked at the correlation between the shear wave velocity measured by wireline logging and predicted from Eq.8 for sandstone and BVG sections in Nirex Borehole RCF3. Laboratory measurements on core samples of shear wave velocity are not routinely practicable. The measurement of V_s in the field has become a routine; however, this work was reviewed in the current study for cases in which field measurements of V_s are not available.

Generally the correlation between wireline measured and predicted shear wave velocity appears to be good, although closer inspection shows sections where correlation is not that good. Within both sandstone and BVG there are sections where velocities change markedly over short intervals. At depths between 407 and 414 m brt in the St Bees Sandstone, measured V_s varied between 1.8 and 2.9 km.s^{-1} whereas predicted V_s only varied between 2.2 and 2.7 km.s^{-1}; this is possibly due to the fact that V_p can be unaltered by fractures under certain conditions, whereas V_s can change. Any prediction stemming from V_p will not observe these effects. Within this same section, porosity derived from measured V_s varies between 0.06 and 0.16, errors in ϕ derived from predicted V_s are up to 0.06 of total porosity (25 % error). Within the BVG similar observations between measured and calculated V_s are observed.

Engelder and Plumb, 1984, showed clear differences between *in situ* measured and laboratory measured seismic velocities. Tests were conducted on Milford Granite, Machias sandstone, Barre granite and Tully limestone, all of which have well defined fabrics. In all tests, the laboratory-derived seismic velocities were lower than the *in situ* derived results with anisotropy also varying. In Machias sandstone, no anisotropy was noted in the field, but clear anisotropy was observed in the laboratory. Anisotropy in the laboratory was also enhanced in Barre granite. This study highlights the difficulty in comparing laboratory and field measurements.

3.6 GRANULAR PARAMETERS

As shown in Table 1 and Figure 2, the parameters of the mineral grains [V_{pg}, ρ_g] are problematic and considerably amplify error. A 5 % variation in V_{pg} and ρ_g results in ~37 % (ϕ = 0.0146 – 0.0323) error in ϕ (×7.4). A value for ρ_g of 2.3555 g.cc^{-1} (~13 % error in bulk rock density) is sufficient to yield a zero porosity estimate. Neither of these parameters are directly measured and are estimated from Eq.5 and Eq.9.

Eq.5 is applied by iteration as ϕ is required. Of the other parameters, ρ_f is prone to error as discussed previously and ρ_b is prone to measurement errors of approximately 1 %. Thus any significant error in ρ_g will derive from the iteration process, which is discussed in Section 3.7.

Eq.9 was determined empirically by Birch, 1961, from a range of silicates, oxides and single crystals, work conducted on pure crystalline material (i.e. well formed material consisting of crystals of only one type) that may be similar to the BVG found at Sellafield. However, the work was conducted on mainly monocrystalline materials (i.e. rock consisting of only one

mineral type such as calcite or quartz) and not polycrystalline materials (i.e. rock consisting of a number of mineral types) as is the case for most successions of the BVG found in the Sellafield area. The granular sandstone material will give a different behaviour. Work on majorite garnets by Gwanmesia *et al.*, 1998, supports the use of this equation. That study was conducted on a well-formed monocrystalline material at pressures far greater (up to 8 GPa) than those in the Nirex boreholes. At these pressures, any material will behave as intact rock because all fractures will have closed. As previously discussed, the presence of cracks will influence elastic wave propagation and in application Eq.9 was altered to:

$$V_{pg} = 2.2\rho_g \qquad \textbf{(11)}$$

This relationship gave a better fit to observed data. The use of Eq.11 reduces the calculated porosity by a relatively constant amount ($\phi \sim 0.0178$). At high porosity values, the difference between porosity calculated using Eq.9 and Eq.11 is less apparent. However, at porosity values less than 0.025 the effect is pronounced. The validity of both Eq.9 and Eq.11 is in question. For sample E57, $\phi = 0.0239$ using Eq.9, whereas $\phi = 0.0134$ using Eq.11.

The predicted ρ_g from acoustic impedance was found to be comparable to that measured directly from 29 sample cores. These predictions were made using Eq.11. Data suggest that the value of ρ_g as estimated from acoustic impedance data tends to be slightly greater than measured ρ_g. Spread about the 1:1 relationship is generally within 1 % error. However, as previously shown, Eq.6 is very sensitive to error derived from ρ_g and even 1 % error in ρ_g will produce approximately 7.4 % error in calculated porosity ($\phi = 0.0257 \pm 0.0089$).

3.7 THE SENSITIVITY OF EQUATION 5 USING ITERATION TO DETERMINE GRANULAR PARAMETERS

Parameters of mineral grains are not easily measured in the borehole environment and an iterative approach must be applied to calculate V_{pg} and ρ_g. An initial estimate of ρ_g is given and iteration produces stable results for V_{pg}, ρ_g and ϕ. Experience in application showed that the iterative cycle was completely insensitive to the initial assumed value of mineral grain density and that a generic value of 2.65 g.cc^{-1} is suitable (Brereton, 1997; Brereton *et al.*, 1996).

Using the example described in Table 1 and an initial starting ρ_g of 2.667 g.cc^{-1} (measured value), porosity was estimated as 0.0387 %, while ρ_g and V_{pg} are 2.73 g.cc^{-1} and 6.53 km.s^{-1} respectively. Using the suggested starting grain-density of 2.65 g.cc^{-1}, the resultant values of ρ_g, V_{pg} and ϕ are 2.73 g.cc^{-1}, 6.54 km.s^{-1} and 0.0413 % respectively. This equates to a 6.7% (0.0026) error in the porosity estimate. This problem is worse in higher grain density samples such as H37. Using the measured values, porosity and grain density are estimated as 0.0627 % and 2.86 g.cc^{-1} respectively. Using the suggested initial value of grain density, porosity and grain density are estimated as 0.0792 % and 2.9 g.cc^{-1} respectively. This equates to a 26 % overestimate of porosity and suggests that the starting grain density in the iterative process does have an effect on the porosity measurement. This is to be expected, as three variables are determined during the iterative process and porosity is present on both side of Eq.6 when Eq.5 is substituted for ρ_g.

Table 4 and Figure 4 show the sensitivity of the iterative Eq.6 to input error for three samples (using Eq.5). As before, 5 % errors are introduced to each parameter with similar q_b and q_g terms. As can be seen, porosity determination is still very sensitive to all input parameters for all three samples. Error amplification is most significant in the lower porosity core sample

H87, where a 5 % decrease in bulk density changes porosity from 0.00267 to <0 (-0.0699). This represents a nominal error amplification of over ×500 times.

Table 5 and Figure 4 show the effect of having $q_g \neq q_b$ by altering the V_p/V_s and V_{pg}/V_{sg} ratios. Values are only altered by approximately 1 %, but this can result in significant errors in the prediction in porosity. This demonstrates that the ratio of V_p to V_s needs to be accurately known and that assuming $V_p/V_s = V_{pg}/V_{sg}$ could potentially be problematic.

The only parameters to be used in Eq.6 when deriving porosity estimates from borehole logging tools are V_p, V_s and ρ_b. Schlumberger quote repeatability of ± 0.2 km.s^{-1} and ± 0.02 g.cc^{-1} for sonic and density logging tools respectively. Table 6 and Figure 4 show the effect these margins of input error have on porosity estimates. For all three examples quoted, it is very easy to achieve a negative porosity result. Standard deviations in total volume of the sample are up to ± 0.03, which when considering these are low porosity rocks, constitutes significant errors. It is not quantitatively meaningful to quote the porosity of sample E57 as 0.01335 ± 0.05 [i.e. a range of porosity from –0.03665 to 0.06335] when high levels of precision are required. However, it is evident that this method of porosity determination may be useful as a relative result, signifying the differences between low and high porosity materials.

3.8 OTHER FACTORS

It has already been discussed that temperature and fracture populations have not been considered. Temperature could have an effect on the pore fluid, while fracture populations will have an effect on seismic velocities in differing amounts. Other factors not considered when applying and testing Eq.6 are anisotropy, scale, and physically what is being measured.

A wide range of geomaterials display anisotropy, in porosity, permeability, conductivity, seismic wave propagation, elastic behaviour, fracture population, tortuosity, density, cementation, etc. This anisotropy can be observed and measured within boreholes, but is often neglected. In terms of seismic velocity, considering an anisotropic material as isotropic will yield a velocity equal to the greatest velocity (first arrival). If considerable anisotropy is present, this velocity will be greater than the average seismic velocity at that point. These overestimates will lead to errors in porosity calculation dependant on the degree of anisotropy. Laboratory-based comparison is then questionable as the seismic velocity in the direction of seismic wave propagation applied in the laboratory measurement may not be the same as that applicable down-hole.

Scale of observation is often a problem in laboratory studies. Samples tend to be taken from intact portions of material, e.g. from intact BVG between fracture zones. Wireline logs measure over larger volumes of material that include these imperfections. Thus, scale of measurement will have an effect on seismic velocities and density measurements.

It may be possible that laboratory-based studies are measuring fundamentally different properties. Effective or connected porosity is of interest to matrix diffusion studies. In the wireline based porosity determinations from acoustic impedance, the porosity is likely to be representative of total porosity (total void space). In laboratory-based measurements, porosity will be that of effective porosity (connected void space, which does not include void space disconnected from other pores). If pores are disconnected, then resaturation methods of porosity measurement will not include these pores, which will have an effect upon acoustic impedance. This shows that wireline measurements may introduce a systematic error if there is a significant component of isolated (non-connected) porosity. Cuss, 1999, showed that porosity measurements made by three different methods yielded different estimates in three

sandstones. Porosity was measured by resaturation, density bottle with crushed material, and using scanning electron microscopy. Porosities estimated by the three methods in Penrith Sandstone varied between 0.252-0.285, in Darley Dale Sandstone the variation was 0.113-0.14%, and in Tennessee Sandstone variation of 0.068-0.078 % was observed. Repeat experimentation showed this variation was not due to geological heterogeneities as porosity is homogeneous within these sandstone types. Thus, ranges of porosity determined are dependent on the measurement methodology. Porosity calculated by scanning electron microscopy was consistently lower than estimates from the other methods. Although these materials are relatively porous, it demonstrates that considerable variations can be observed if measurements are aimed at both total and effective porosity. In low permeability rocks connectivity of pores may be low, resulting in considerable differences between effective and total porosity. Brereton, 1997, showed considerable difference between laboratory measured porosity and porosity derived from wireline logging methods (both using Eq.6 and neutron porosity logs). Differences in porosity were as great as 0.1 (up to 50 % error) in the St. Bees Sandstone and 0.05 (up to 50 % error) in the BVG. Generally, correlation was better in the more porous St. Bees Sandstone than in the lower porosity BVG. This could be a direct result of pore connectivity.

4 Conclusions

This report highlights the problems of taking theoretical work to the limits of its practical implementation. A major problem is that the key focus of the Nirex investigations in the Sellafield area was on crystalline rocks with typically less than five per cent porosity. In such rocks a change of as little as one per cent porosity can have significant impact on fluid migration and permeability properties.

The basic logging suite run in the Nirex deep boreholes, although of the highest standard in the industry, could be enhanced in key target zones by careful depth matching and a shorter depth interval for recording parameters. The wireline tools are designed for the hydrocarbon industry and are therefore not ideal for crystalline rocks.

It has been shown that the key Eq.6 is very sensitive to errors inherent within all parameters. Assuming each relationship is valid, unacceptably large errors are seen in porosity estimation from expected input errors. Errors in porosity estimation derived from error in only one parameter can be as great as $\phi = 0.013 \pm 0.03$ (i.e. 230% error; sample E57), $\phi = 0.033 \pm 0.03$ % (i.e. 90% error; sample G72), and $\phi = 0.003 \pm 0.03$ % (i.e. 1000% error; sample H87). This shows that uncertainty in porosity increases as porosity decreases. The point at which this method becomes useful, i.e. ≡ detection limit, is dependent on the resolution required. Porosity estimation from wireline logs should be of good quality for porous materials with porosity greater than 0.1. Unfortunately, the measurements on core from the Nirex boreholes do not provide laboratory data of sufficient quality to adequately test Eq.6.

Sonic and gamma density logging tools generally have repeatability of 2 and 1 % respectively. This shows that measured V_p and ρ_b can be considered to be accurate to within these error margins. However, these margins of error will result in inaccuracies of 16 and 8 % error in ϕ respectively at low porosities (i.e. ~ 0.024).

The compressibility modulus, q, had previously been introduced separately for bulk rock (q_b) and mineral grain (q_g). This assumption is invalid as influences such as fracture population

and the nature of pore fluids can alter bulk rock q, by increasing or decreasing a, while unchanging q_g.

Shear velocity predicted from Eq.7 was shown to give large discrepancies that result in significant errors in ϕ.

Porosity estimates are very sensitive to errors in the parameters of solid grains forming the rock matrix (V_{pg}, V_{sg}, and ρ_g). The use of Eq.9 is questionable.

The iterative approach to determining granular properties (ρ_g and V_{pg}) and porosity (ϕ) was seen to be sensitive to the initial estimate of grain density. These margins of error on porosity were deemed too severe for meaningful use if high precision is required.

The general conclusion is that the theoretical work previously done to calibrate porosity with the acoustic impedance of a rock should be limited in practice to rocks whose porosity is greater than that seen in the BVG in the Sellafield area ($\phi \sim 0.05$). At lower porosities, the estimates should be only used as a relative and not an absolute indicator.

	V_p (km.s^{-1})	V_{pg} (km.s^{-1})	V_p/V_s	V_f (km.s^{-1})	ρ_b (g.cc^{-1})	ρ_g (g.cc^{-1})	ρ_f (g.cc^{-1})	ϕ	$\delta\phi$ (%)	$\delta\phi$	Amplification of input error	Varying parameter
	5.62	**6.351**	**0.56**	**1.5544**	**2.662**	**2.667**	**1.05**	**0.0239**				
1	*5.339*	6.351	0.56	1.5544	2.662	2.667	1.05	0.0364	44.42	0.0107	×8.4	V_p
2	*5.901*	6.351	0.56	1.5544	2.662	2.667	1.05	0.0143	-40.54	-0.0097	×8.4	V_p
3	5.62	*6.0335*	0.56	1.5544	2.662	2.667	1.05	0.0146	-39.23	-0.0094	×7.4	V_{pg}
4	5.62	*6.6686*	0.56	1.5544	2.662	2.667	1.05	0.0323	34.86	0.0084	×7.4	V_{pg}
5	5.62	6.351	*0.49*	1.5544	2.662	2.667	1.05	0.0206	-14.12	-0.0034	×1.6	V_p/V_s
6	5.62	6.351	*0.532*	1.5544	2.662	2.667	1.05	0.0224	-6.401	-0.0015	×1.6	V_p/V_s
7	5.62	6.351	*0.588*	1.5544	2.662	2.667	1.05	0.0258	7.745	0.0019	×1.6	V_p/V_s
8	5.62	6.351	*0.68*	1.5544	2.662	2.667	1.05	0.0359	49.88	0.0120	×1.6	V_p/V_s
9	5.62	6.351	0.56	*1.4766*	2.662	2.667	1.05	0.0227	-5.452	-0.0013	×1.1	V_f
10	5.62	6.351	0.56	*1.6321*	2.662	2.667	1.05	0.0253	5.504	0.0013	×1.1	V_f
11	5.62	6.351	0.56	1.5544	*2.529*	2.667	1.05	0.0346	44.42	0.0107	×8.5	ρ_b
12	5.62	6.351	0.56	1.5544	*2.795*	2.667	1.05	0.0143	-40.54	-0.0097	×8.5	ρ_b
13	5.62	6.351	0.56	1.5544	2.662	*2.534*	1.05	0.0146	-39.23	-0.0094	×7.4	ρ_g
14	5.62	6.351	0.56	1.5544	2.662	*2.801*	1.05	0.0323	34.86	0.0084	×7.4	ρ_g
15	5.62	6.351	0.56	1.5544	2.662	2.667	*0.998*	0.0215	-10.39	-0.0025	×2.2	ρ_f
16	5.62	6.351	0.56	1.5544	2.662	2.667	*1.103*	0.0267	11.13	0.0027	×2.2	ρ_f

Table 1 Test of sensitivity of Eq.6 to each parameter with ± 5 % error. The amplification of input error shows that ± 5 % error in V_p is amplified 8.4 times to ± 42% error in porosity prediction. The grey highlighted table cells illustrate which parameter is being varied, the bold characters illustrate the starting parameters for sample E57.

q_b	q_g	ϕ	$\delta\phi$ (%)	$\delta\phi$	Amplification of input error	Varying parameter
0.7186	**0.7186**	**0.0239**				
0.7545	0.7186	0.0282	17.40	0.0042	×3.5	q_b
0.6827	0.7186	0.0198	-17.55	-0.0042	×3.5	q_g
0.6827	*0.7545*	0.0160	-33.18	-0.0079	×6.5	q_b & q_g

Table 2 The effect of assigning different values for q_b and q_g in Eq.6. Example parameters are as in Table 1 with V_p = 5.62 km.s^{-1}, V_{pg} = 6.351 km.s^{-1}, V_p/V_{sg} = 0.56, V_f = 1.5544 km.s^{-1}, ρ_b = 2.662 g.cc^{-1}, ρ_g = 2.667 g.cc^{-1}, ρ_f = 1.05 g.cc^{-1}. The grey highlighted table cells illustrate which parameter is being varied, the bold characters illustrate the starting parameters for sample E57.

	Input Error (%)	V_p ($km.s^{-1}$)	V_s ($km.s^{-1}$)	ρ_b ($g.cc^{-1}$)	ϕ	$\delta\phi$ (%)	$\delta\phi$	Amplification of input error	Varying parameter
		5.62	**3.1472**	**2.662**	**0.0239**				
1	3.44	*5.82*	3.1472	2.662	0.0078	-67.3	0.0161	× 19.6	V_p
2	3.44	*5.42*	3.1472	2.662	0.0431	79.6	-0.0191	× 23.2	V_p
3	6.35	5.62	3.3472	2.662	0.0444	85.2	0.0204	× 13.4	V_s
4	6.35	5.62	2.9472	2.662	0.0074	-69.1	-0.0166	× 10.9	V_s
5	0.75	5.62	3.1472	2.682	0.0225	-6.33	-0.0015	× 8.4	ρ_b
6	0.75	5.62	3.1472	2.642	0.0255	6.41	0.0015	× 8.5	ρ_b

Table 3 Test of sensitivity of Eq.6 to each parameter measured in the field with errors quoted by Schlumberger. Velocity and density measurements have errors of ± 0.2 $km.s^{-1}$ and ± 0.02 $g.cc^{-1}$ respectively. The grey highlighted table cells illustrate which parameter is being varied, the bold characters illustrate the starting parameters for sample E57.

Parameter	Linear error amplification	Non-linear error amplification										
		0.5	1	1.5	2	2.5	3	3.5	4	4.5	5	Power Law
V_p	× 8.5	/	/	/	/	/	/	/	/	/	/	/
ρ_b	× 8.5	/	/	/	/	/	/	/	/	/	/	/
V_f	× 1.1	/	/	/	/	/	/	/	/	/	/	/
V_{pg}	× 7.4	/	/	/	/	/	/	/	/	/	/	/
ρ_f	× 1.1	/	/	/	/	/	/	/	/	/	/	/
ρ_g	× 7.4	/	/	/	/	/	/	/	/	/	/	/
V_p/V_s	× 1.4	/	/	/	/	/	/	/	/	/	/	/
V_p/V_s^*	/	× 64	× 32	× 21	× 16	× 13	× 11	× 9.1	× 8.0	× 7.1	× 6.4	65.8 x^{-1}
q_b	/	× 35	× 18	× 12	× 8.7	× 7.0	× 5.8	× 5.0	× 4.4	× 3.9	× 3.5	35.1 x^{-1}
q_g	/	× 35	× 18	× 12	× 8.8	× 7.0	× 5.9	× 5.0	× 4.4	× 3.9	× 3.5	35.1 x^{-1}

Table 4 The amplification of mathematical error through Eq.6 for varying input errors. The parameters of V_p/V_s, q_b and q_g have a decaying error amplification response to input error. All other parameters have a linear response of input error to output error amplification.

Sample	V_p (km.s^{-1})	V_s (km.s^{-1})	ρ_b (g.cc^{-1})	ρ_f (g.cc^{-1})	V_f (km.s^{-1})	ρ_{gstart} (g.cc^{-1})	ρ_g (g.cc^{-1})	V_{pg} (km.s^{-1})	ϕ	$\delta\phi$ (%)	$\delta\phi$	Amplification of input error	Varying parameter
E57	**5.62**	**3.147**	**2.662**	**1.05**	**1.554**	**2.667**	**0.0268**	*5.904*	**0.0134**				
	5.339	3.147	2.662	1.05	1.554	2.667	0.0271	5.970	0.0310	132.5	0.0177	×27	V_p
	5.901	3.147	2.662	1.05	1.554	2.667	0.0266	5.844	-0.0036	-126.8	-0.0169	×25	V_p
	5.62	*3.305*	2.662	1.05	1.554	2.667	0.0272	6.000	0.0391	193.1	0.0258	×39	V_s
	5.62	*2.989*	2.662	1.05	1.554	2.667	0.0265	5.820	-0.0103	-177.5	-0.0237	×36	V_s
	5.62	3.147	*2.529*	1.05	1.554	2.667	0.0245	5.390	-0.0568	-525.5	-0.0702	×105	ρ_b
	5.62	3.147	*2.795*	1.05	1.554	2.667	0.0289	6.309	0.0399	198.8	0.0265	×40	ρ_b
	5.62	3.147	2.662	*0.998*	1.554	2.667	0.0268	5.898	0.0114	-14.91	-0.002	×3.0	ρ_f
	5.62	3.147	2.662	*1.103*	1.554	2.667	0.0269	5.911	0.0157	17.30	0.0023	×3.5	ρ_f
	5.62	3.147	2.662	1.05	*1.477*	2.667	0.0268	5.900	0.0122	-8.914	-0.0012	×1.8	V_f
	5.62	3.147	2.662	1.05	*1.632*	2.667	0.0269	5.910	0.0146	9.663	0.0013	×1.9	V_f
	5.62	3.147	2.662	1.05	1.554	*2.534*	0.0272	5.970	0.0317	137.5	0.0184	×28	ρ_{gstart}
	5.62	3.147	2.662	1.05	1.554	*2.807*	0.0263	5.789	-0.0192	-244.4	-0.0326	×49	ρ_{gstart}
G72	**5.24**	**2.934**	**2.687**	**1.05**	**1.554**	**2.738**	**0.0274**	**6.034**	**0.0330**				
	5.502	2.934	2.687	1.05	1.554	2.738	0.0271	5.969	0.0157	-52.38	-0.0173	×11	V_p
	4.978	2.934	2.687	1.05	1.554	2.738	0.0278	6.105	0.0511	54.68	0.0181	×11	V_p
	5.24	*3.081*	2.687	1.05	1.554	2.738	0.0279	6.137	0.0589	78.70	0.0260	×16	V_s
	5.24	*2.788*	2.687	1.05	1.554	2.738	0.0270	5.944	0.0091	-72.46	-0.0239	×15	V_s
	5.24	2.934	*2.821*	1.05	1.554	2.738	0.0293	6.440	0.0565	71.01	0.0234	×14	ρ_b
	5.24	2.934	*2.553*	1.05	1.554	2.738	0.0251	5.528	-0.0278	-184.1	-0.0608	×37	ρ_b
	5.24	2.934	2.687	*1.102*	1.554	2.738	0.0275	6.051	0.0386	16.78	0.0055	×3.4	ρ_f
	5.24	2.934	2.687	*0.998*	1.554	2.738	0.0274	6.019	0.0282	-14.60	-0.0048	×2.9	ρ_f
	5.24	2.934	2.687	1.05	*1.477*	2.738	0.0274	6.023	0.0302	-8.66	-0.0029	×1.7	V_f
	5.24	2.934	2.687	1.05	*1.632*	2.738	0.0275	6.046	0.0361	9.331	0.0031	×1.9	V_f
	5.24	2.934	2.687	1.05	1.554	*2.875*	0.0269	5.930	0.0049	-84.88	-0.0280	×17	ρ_{gstart}
	5.24	2.934	2.687	1.05	1.554	*2.601*	0.0277	6.101	0.0501	51.83	0.0171	×10	ρ_{gstart}
H87	**5.92**	**3.315**	**2.719**	**1.05**	**1.554**	**2.723**	**0.0272**	**5.992**	**0.0027**				
	6.216	3.315	2.719	1.05	1.554	2.723	0.0269	5.934	-0.0131	-592.1	-0.0158	×120	V_p
	5.624	3.315	2.719	1.05	1.554	2.723	0.0275	6.054	0.0193	620.9	0.0166	×120	V_p
	5.92	*3.481*	2.719	1.05	1.554	2.723	0.0277	6.084	0.0270	912.0	0.0244	×180	V_s
	5.92	*3.149*	2.719	1.05	1.554	2.723	0.0269	5.911	-0.0196	-832.2	-0.0222	×170	V_s
	5.92	3.315	*2.855*	1.05	1.554	2.723	0.0291	6.403	0.0299	1020	0.0272	×200	ρ_b
	5.92	3.315	*2.583*	1.05	1.554	2.723	0.0248	5.464	-0.0699	-2718	-0.0726	×540	ρ_b
	5.92	3.315	2.719	*1.103*	1.554	2.723	0.0272	5.993	0.0031	17.60	0.0005	×3.5	ρ_f
	5.92	3.315	2.719	*0.998*	1.554	2.723	0.0272	5.990	0.0023	-14.61	-0.0004	×2.9	ρ_f
	5.92	3.315	2.719	1.05	*1.477*	2.723	0.0272	5.991	0.0024	-8.614	-0.0002	×1.7	V_f
	5.92	3.315	2.719	1.05	*1.632*	2.723	0.0272	5.993	0.0029	9.738	0.0002	×1.9	V_f
	5.92	3.315	2.719	1.05	1.554	*2.859*	0.0267	5.881	-0.0287	-1162	-0.0310	×230	ρ_{gstart}
	5.92	3.315	2.719	1.05	1.554	*2.587*	0.0276	6.061	0.0212	694.4	0.0185	×140	ρ_{gstart}

Table 5 Test of sensitivity of Eq.6 to each parameter with ± 5 % error using the iterative approach to determining ρ_g, V_{pg} and ϕ. Examples are given for sample E57 (as in Tables 1-3) and for samples G72 and H87.

Sample	V_p/V_s	V_{pg}/V_{sg}	ρ_g ($g.cc^{-1}$)	V_{pg} ($km.s^{-1}$)	ϕ	$\delta\phi$ (%)	$\delta\phi$	*Varying parameter*
H87	**0.56**	**0.56**	**2.724**	**5.992**	**0.0027**			
	0.56	0.57	0.709	5.959	-0.0063	-340	-0.0090	V_{pg}/V_{sg}
	0.57	0.56	2.738	6.023	0.0111	310	0.0084	V_p/V_s
	0.56	0.55	2.736	6.019	0.0102	280	0.0075	V_{pg}/V_{sg}
	0.55	0.56	2.710	5.962	-0.0055	-305	-0.0082	V_p/V_s
	0.55	0.57	2.694	5.927	-0.0152	-670	-0.0178	V_p/V_s & $_{pg}/V_{sg}$
	0.57	0.55	2.750	6.050	0.0181	580	0.0155	V_p/V_s & $_{pg}/V_{sg}$
G72	**0.56**	**0.56**	**2.743**	**6.034**	**0.0330**			
	0.56	0.57	2.729	6.003	0.0248	-25	-0.0082	V_{pg}/V_{sg}
	0.57	0.56	2.759	6.069	0.0420	27	0.0090	V_p/V_s
	0.56	0.55	2.755	6.061	0.0399	21	0.0069	V_{pg}/V_{sg}
	0.55	0.56	2.728	6.000	0.0243	-27	-0.0088	V_p/V_s
	0.55	0.57	2.713	5.968	0.0154	-53	-0.0177	V_p/V_s & $_{pg}/V_{sg}$
	0.57	0.55	2.770	6.095	0.0484	47	0.0154	V_p/V_s & $_{pg}/V_{sg}$
E57	**0.56**	**0.56**	**2.684**	**5.904**	**0.0134**			
	0.56	0.57	2.669	5.872	0.0045	-66	-0.0088	V_{pg}/V_{sg}
	0.57	0.56	2.699	5.937	0.0223	67	0.0089	V_p/V_s
	0.56	0.55	2.696	5.932	0.0208	56	0.0074	V_{pg}/V_{sg}
	0.55	0.56	2.669	5.873	0.0047	-65	-0.0087	V_p/V_s
	0.55	0.57	2.654	5.839	-0.0049	-140	-0.0183	V_p/V_s & $_{pg}/V_{sg}$
	0.57	0.55	2.710	5.963	0.0292	120	0.0159	V_p/V_s & $_{pg}/V_{sg}$

Table 6 The effect of assigning different values for q_b and q_g in Eq.6 during the iterative cycle.

	V_p (km.s^{-1})	V_s (km.s^{-1})	ρ_b (g.cc^{-1})	ρ_f (g.cc^{-1})	V_{PS} (km.s^{-1})	ϕ	$\delta\phi$ (%)	$\delta\phi$	Amplification of input error	Varying parameter
E57	**5.62**	**3.147**	**2.662**	**2.684**	**5.904**	**0.0134**				
	5.82	3.147	2.662	2.664	5.861	0.0012	-90.79	-0.0121	× -26	V_p
	5.42	3.147	2.662	2.705	5.951	0.0259	93.71	0.0125	× -26	V_p
	5.62	*3.347*	2.662	2.741	6.030	0.0465	248.6	0.0332	× 39	V_s
	5.62	*2.947*	2.662	2.636	5.799	-0.0165	-223.3	-0.0298	× 35	V_s
	5.62	3.147	*2.682*	2.713	5.969	0.0187	39.85	0.0053	× 53	ρ_b
	5.62	3.147	*2.642*	2.654	5.838	0.0073	-45.32	-0.0061	× 60	ρ_b
G72	**5.24**	**2.934**	**2.687**	**2.743**	**6.034**	**0.0330**				
	5.44	2.934	2.687	2.720	5.984	0.0198	-40.17	-0.0133	× -11	V_p
	5.04	2.934	2.687	2.767	6.087	0.0467	41.50	0.0137	× -11	V_p
	5.24	*3.134*	2.687	2.808	6.179	0.0691	109.2	0.0360	× 16	V_s
	5.24	*2.734*	2.687	2.688	5.914	0.0008	-97.49	-0.0322	× 14	V_s
	5.24	2.934	*2.707*	2.772	6.098	0.0377	14.15	0.0047	× 19	ρ_b
	5.24	2.934	*2.667*	2.713	5.969	0.0277	-16.06	-0.0053	× 22	ρ_b
H87	**5.92**	**3.315**	**2.719**	**2.723**	**5.992**	**0.0027**				
	6.12	3.315	2.719	2.706	5.952	-0.0081	-402.6	-0.0108	× -120	V_p
	5.72	3.315	2.719	2.742	6.033	0.0138	416.1	0.0111	× -120	V_p
	5.92	*3.515*	2.719	2.775	6.105	0.0324	1111	0.0297	× 180	V_s
	5.92	*3.115*	2.719	2.680	5.896	-0.0239	-995.9	-0.0270	× 170	V_s
	5.92	3.315	*2.739*	2.753	6.056	0.0080	200.4	0.0054	× 270	ρ_b
	5.92	3.315	*2.699*	2.693	5.926	-0.0034	-227	-0.0061	× 310	ρ_b

Table 7 Test of sensitivity of Eq.6 to each parameter measured in the field with errors quoted by Schlumberger. Velocity and density measurements have errors of ± 0.2 km.s^{-1} and ± 0.02 g.cc^{-1} respectively.

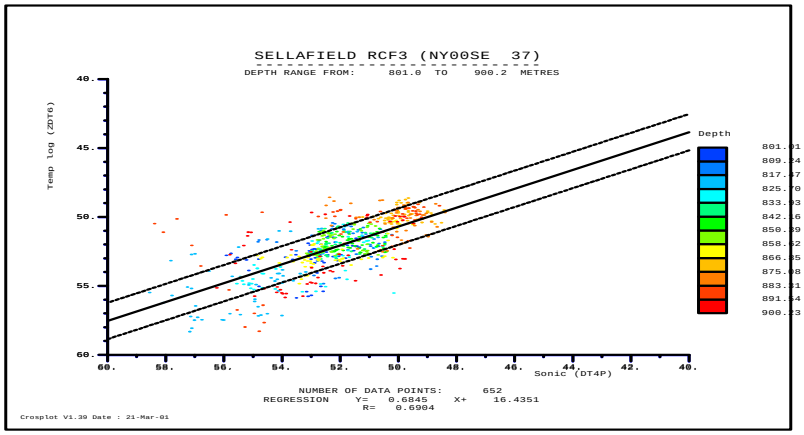

Figure 1d: Depth shift of 1.0m

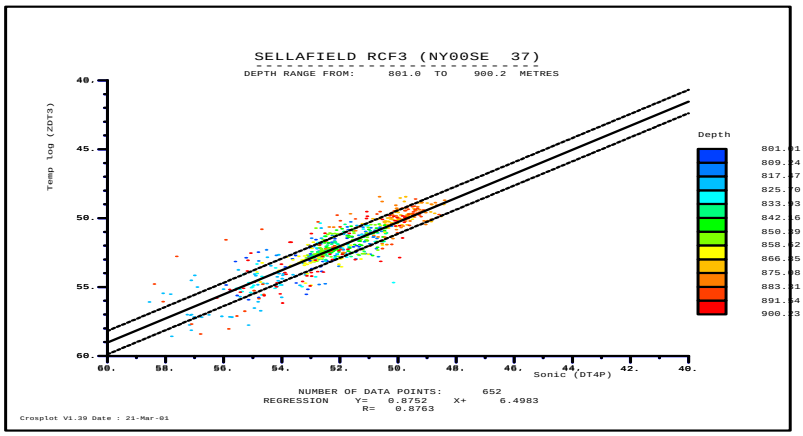

Figure 1c: Depth shift of 0.45m

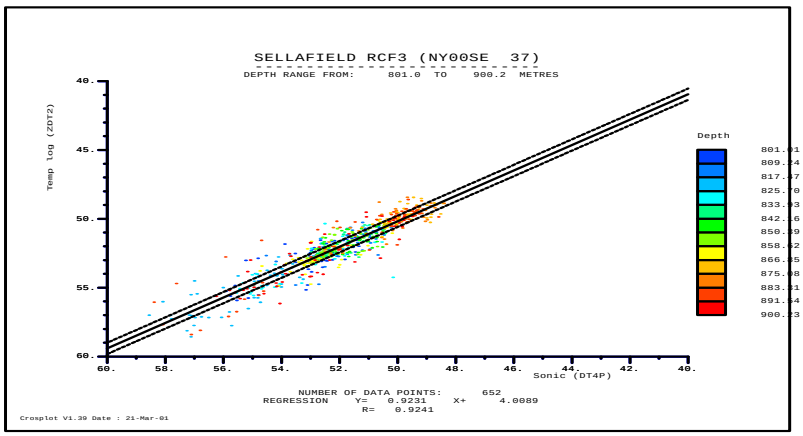

Figure 1b: Depth shift of 0.3m

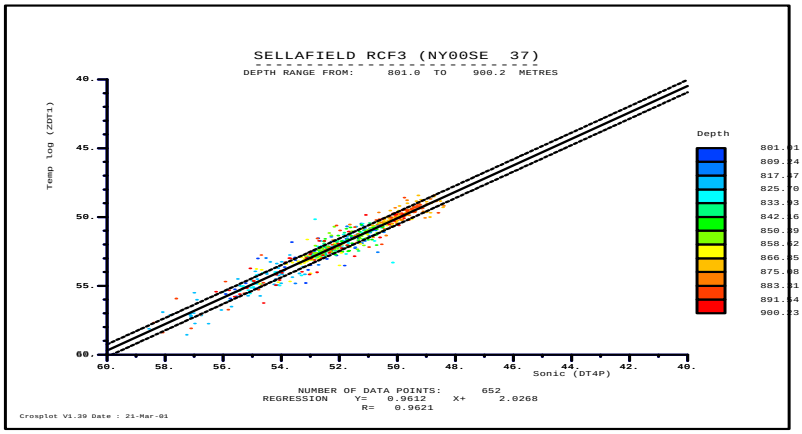

Figure 1a: Depth shift of 0.1m

Figure 1 Crossplots of a sonic log plotted against the same log depth shifted by amount denoted below. From 1a to 1d a decrease in linearity occurs, and a greater spread in the standard deviation as the depth is shifted.

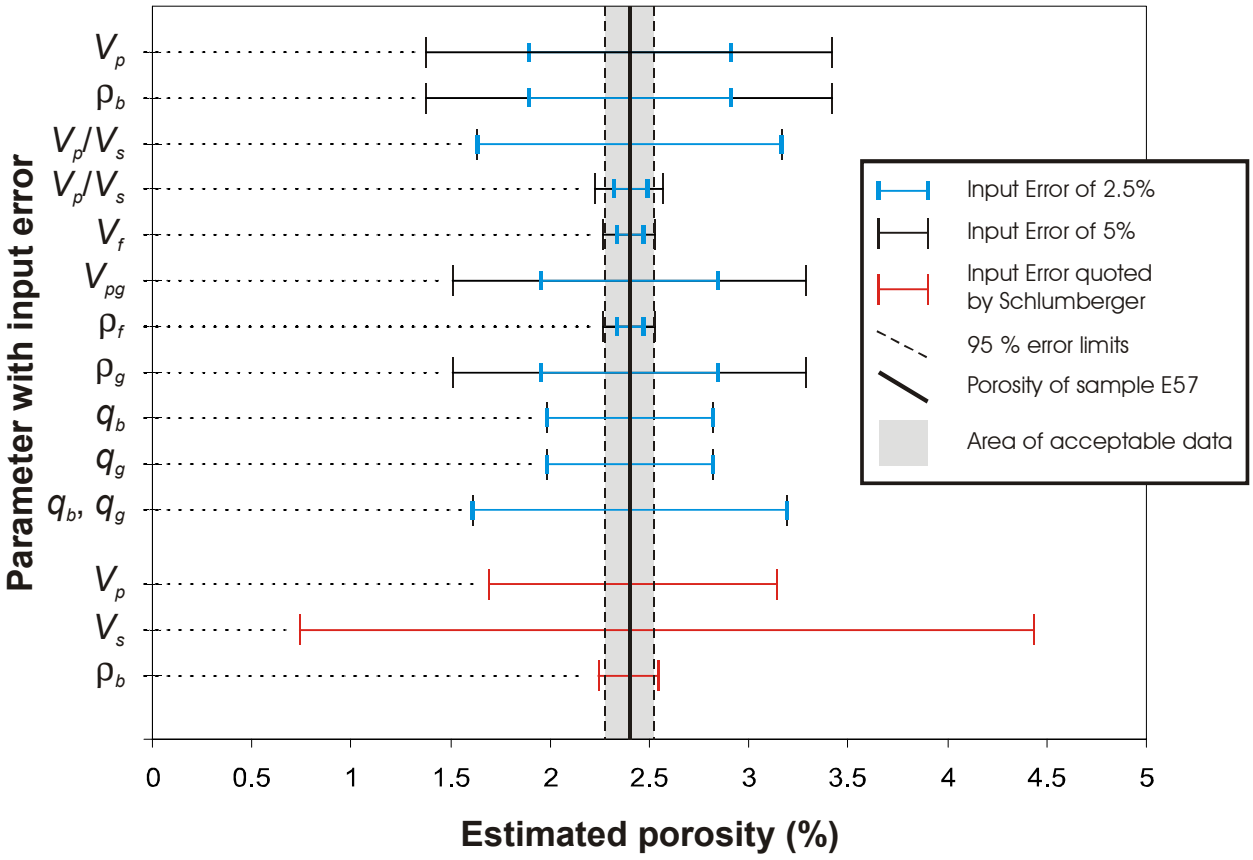

Figure 2 Error in porosity estimate using Eq.6 for input errors of 2.5%, 5% and the error quoted by Schlumberger. This graph shows the data displayed in Table 1, Table 2, and Table 3.

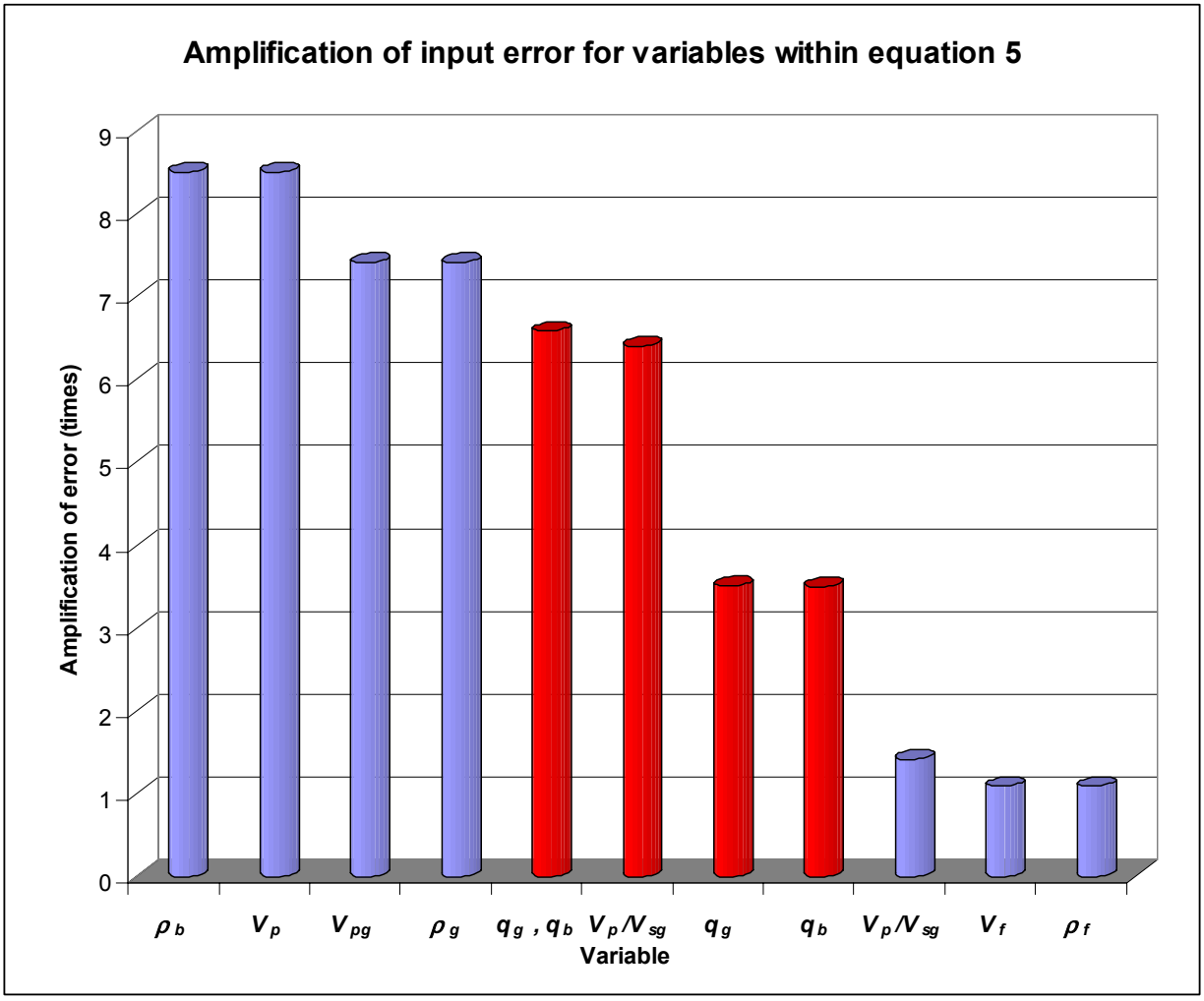

Figure 3 The amplification of input error in Eq.6. Red columns have non-linear (Power Law) response to input errors (see Table 4).

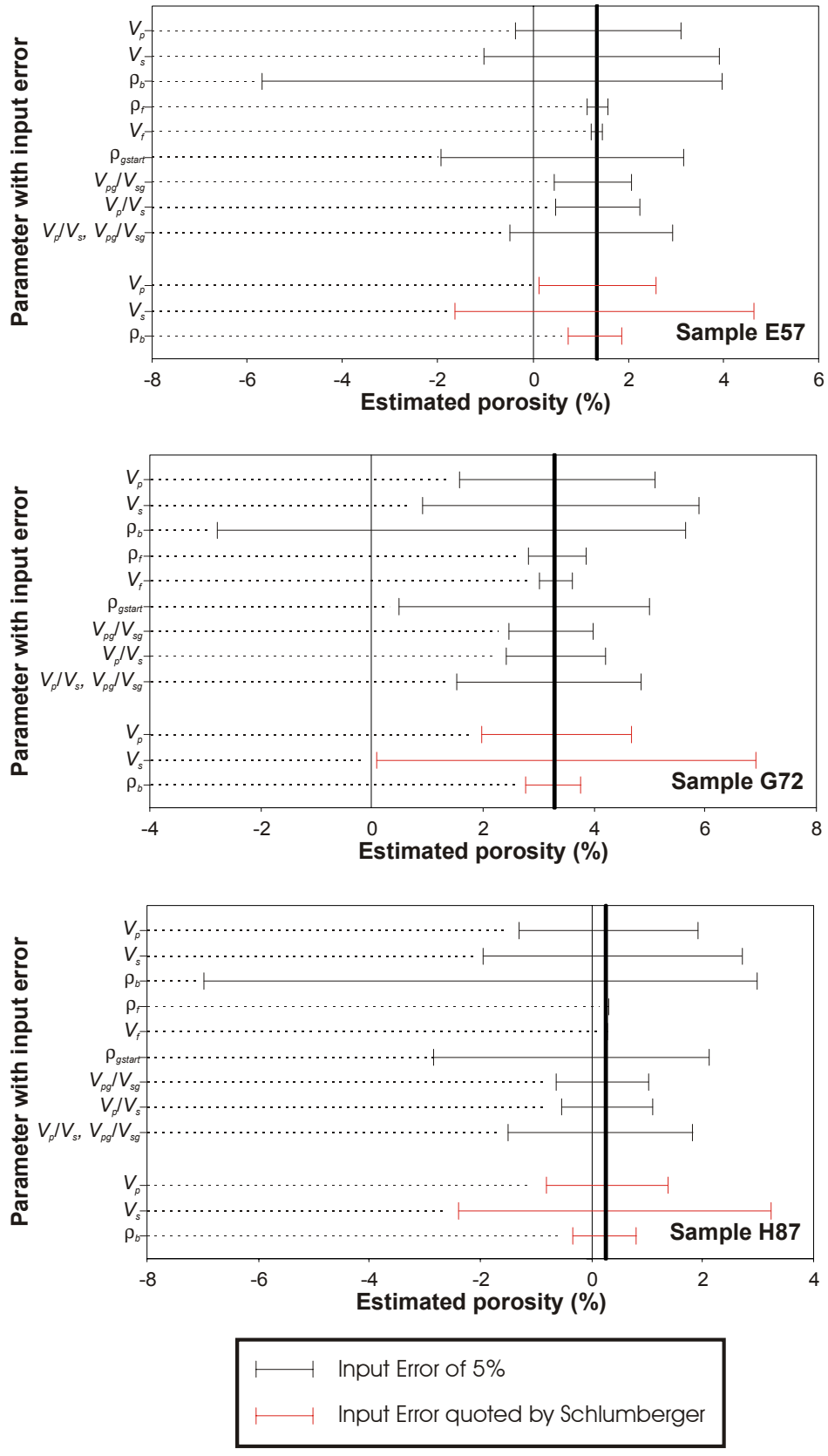

Figure 4 Error in porosity estimate using iterative Eq.6 for input errors of 5 % and the error quoted by Schlumberger. This graph shows the data displayed in Table 1, Table 2, and Table 3

References

Most of the references listed below are held in the Library of the British Geological Survey at Keyworth, Nottingham. Copies of the references may be purchased from the Library subject to the current copyright legislation.

Anderson, D.L., Minster, B., and Cole, D. (1974). The effect of orientated cracks on seismic velocities: J. Geophys. Res., 79, pp. 4011-4015.

Birch, F. (1960). The velocity of compressional waves in rocks to 10 kilobars - Part 1: Journal of Geophysical Research, 65, pp. 1083-1102.

Birch, F. (1961). The velocity of compressional waves in rocks to 10 kilobars - Part 2: Journal of Geophysical Research, 66, pp. 2199-2224.

Brereton, N.R. (1997). Porosity, permeability and the scale of measurement - an integrated approach to rock mass property predictions. British Geological Survey Report WK/97/14

Brereton, N.R., Jackson, P.D., Jefferies, N.L., and Swanton, S.W. (1996). The suitability of wireline logs for evaluating the matrix diffusion properties of in situ rock. AEA Technology Report AEAT/ERRA - 0322 A report produced for United Kingdon Nirex Limited

Christensen, N.I. (1996). Poisson's ratio and crustal seismology: Journal of Geophysical Research, 101, pp. 3139-3156.

Cuss, R.J. (1999). An experimental investigation of the mechanical behaviour of sandstones with reference to borehole stability Ph.D. thesis: Manchester, UK, University of Manchester.

Ellis, D.V. (1987). Well logging for Earth Scientists: New York, Elsevier.

Engelder, T., and Plumb, R. (1984). Changes in In Situ Ultrasonic Properties of Rock on Strain Relaxation: Int. J. Rock Mech. Min. Sci. & Geomech. Abstr., 21, pp. 75-82.

Gwanmesia, G.D., Chen, G., and Liebermann, R.C. (1998). Sound velocities in MgSiO3-garnet to 8 GPa: Geophysical Research Letters, 25, pp. 4553-4556.

Hadley, K. (1975). Vp/Vs anomalies in dilatant rock samples: Pure and Applied Geophysics, 113, pp. 1-23.

Jones, M.J., McCann, C., Astin, T.R., and Sothcott, J. (1998). The effects of pore fluid salinity on ultrasonic wave propagation in sandstones: Geophysics, 63, pp. 928-934.

Keys, W.S. (1997). A practical guide to borehole geophysics in environmental investigations: Boca Raton, CRC Lewis Publishers.

Log Analyst (1994). Special Issue on Core Analysis: Log Analyst, 35 (3).

NIREX (1997). Spatial heterogeneity of rock mass properties. UK NIREX Ltd. Report No. SA/97/021

Nur, A., and Simmons, G. (1969). The effect of saturation on velocity in low porosity rocks: Earth Planet. Sci. Lett., 7, pp. 183-193.

Paterson, M.S. (1978). Experimental Rock Deformation - The Brittle Field.: Berlin, Springer-Verlag, 254 pp.

Rogers, P.S.Z., and Pitzer, K.S. (1982). Volumetric properties of aqueous sodium chloride solutions: Journal of Physical and Chemical Reference Data, 11, pp. 15-81.

Schlumberger (1989). Log interpretation principles/applications. Schlumberger Schlumberger Educational Services